Functional Materials 19, No.3 (2012)

The formation of *J*-aggregates in solutions of reverse micelles

I.I.Fylymonova, S.L.Yefimova, A.V.Sorokin

Institute for Scintillation Materials, STC "Institute for Single Crystals", National Academy of Sciences of Ukraine, 60 Lenin Ave., 61001 Kharkiv, Ukraine

Received June 15, 2012

Features of BIC *J*-aggregate formation in AOT reverse micelles have been studied using steady-state absorption and luminescence spectroscopy and time-resolved luminescence spectroscopy. BIC *J*-aggregates reveal spherical structure with diameter ~ 20 nm and significant thermal stability. RM diameter decrease results in strong static disorder increase leading to *J*-aggregate band (*J*-band) widening and luminescence quenching. Due to high thermal stability BIC *J*-aggregates are embedded into RM as a whole at any temperatures of stock water solution. Decrease of stock water solution temperature leads to *J*-band narrowing and intensity increasing due to static disorder decreasing.

Исследованы особенности формирования *J*-агрегатов BIC в растворах обратных мицелл (ОМ) с помощью стационарных спектроскопии оптического поглощения и люминесцентной спектроскопии, а также люминесцентной спектроскопии с временным разрешением. *J*-агрегаты BIC имеют сферическую геометрию с диаметром порядка 20 нм и значительную температурную стабильность. Уменьшение диаметра обратных мицелл приводит к увеличению статического беспорядка, в результате чего происходит уширение *J*-полосы и увеличение интенсивности люминесценции. Благодаря высокой температурной стабильности, *J*-агрегаты BIC встраиваются в ОМ при любых температурах исходного раствора. Уменьшение температуры исходного раствора приводит к сужению *J*-полосы и увеличению её интенсивности вследствие уменьшения статического беспорядка.

1. Introduction

Aggregation processes of dye molecules belonging to the class of cyanines have attracted much attention in a wide variety of fields such as nonlinear optics, optoelectronics, photovoltaics, photochemistry, biology and others [1]. This is caused by unique optical properties of cyanine molecular aggregates called *J*-aggregates due to Frenkel excitons formation in well-ordered molecular chains [2–6]. One of the questions in *J*-aggregates photophysics is an influence of different structuring substances such as surfactants, molecular templates, salts and others on optical properties of *J*-aggregates. Recently we have published some results concerning cationic surfactant shell formation around *J*-aggregates of several cyanine dyes [7–11]. Briefly such *J*-aggregates-surfactant complex formation leads to excitonic band (*J*-band) narrowing and increasing, quantum yield enhancement, exciton self-trapping suppression and exciton transport efficiency increasing [7–11]. But our attempts to reproduce such results for anionic dyes *J*-aggregates we were unsuccessful.

In other hand we find reports concerning anionic cyanine dye *J*-aggregation within reverse micelles [12–15]. Reverse micelles (RM) are being widely used as nanoreactors for synthesis of various inorganic nanoparticles with a desired size [16–18]. They are representing water droplets in nonpolar solvent stabilized by surfactants [16–18]. The amount of water dissolved in RMs determines most of the physical and chemical properties of the micellar environment. Size

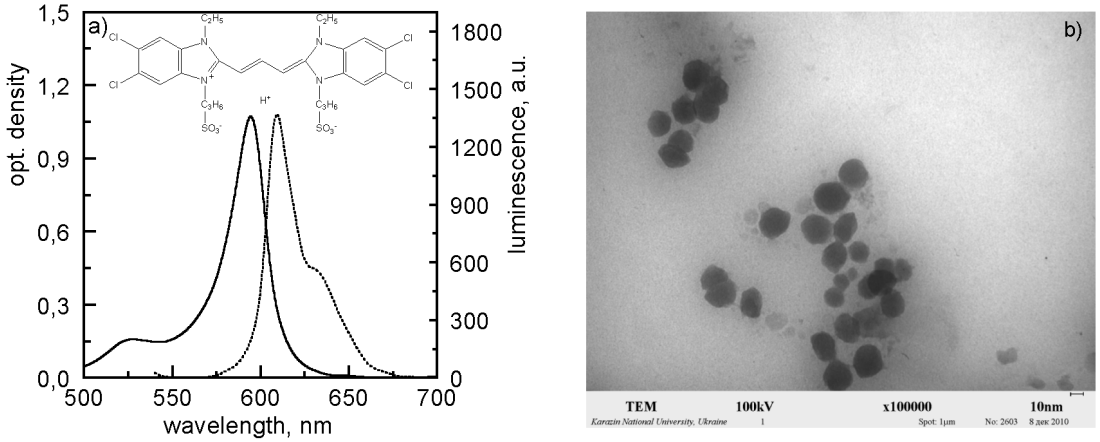

Fig. 1. (a) BIC *J*-aggregates absorption and luminescence (λ_{exc} = 530 nm) spectra. On inset — the dye structure. (b) BIC *J*-aggregates TEM image.

of reverse micelles is controlled by the ratio of $w_0 = [H_2O]/[\text{surfactant}]$, where w_0 determines the average micellar radius and the average number of molecules of water and surfactant in the micelle [16–18].

Investigations directed to *J*-aggregates formation within RMs are reported in only a few works and only for one type of anionic cyanine dye namely 3,3′-di-(γ-sulfopropyl)-4,5,4′,5′-dibenzo-9-ethylthiacarbocyanine dye (DEC) [12–15]. According to the reports the *J*-band becomes wider for *J*-aggregates formed in RM with *J*-band width narrowing at RM diameter increasing [12–15]. If some authors argue that in the first place the spatial restrictions affects the structural quality of aggregates [12, 13], others have suggested direct limiting the size of aggregates and proposed to use the RMs as "molecular sieves" for *J*-aggregates [14, 15]. If w_0 is too small then *J*-aggregates precipitated and at for larger RM diameters *J*-aggregates become stabilized [12–15]. Besides, on the one hand, the aggregates formation in RM is seems to be impossible if the concentration of the dye is much less than RM concentration, on the other hand, the *J*-aggregates formation was observed in RM for a case then an average number of dye molecules in the micelle is much smaller than unity [12–15].

Therefore, the aim of this paper was to study the features of *J*-aggregates formation in reverse micelles to resolve all contradictions. For the *J*-aggregates formation anionic cyanine dye BIC and surfactant AOT were chosen.

2. Experimental

BIC dye (1,1′-diethyl-3,3′-bis-(3-sulfopropyl)-5,5′,6,6′-tetrachlorobenzimidazolocarbocyanine, Fig. 1a, inset) was synthesized by Dr.I.A.Borovoy (Institute for Scintillation Materials NAS of Ukraine) with purity controlled by NMR and thin layer chromatography. AOT [sodium 1,4-bis(2-ethylhexyl)sulfosuccinate] was purchased Aldrich (USA) and used as-received. As a non-polar solvent hexane ($CH_3(CH_2)_4CH_3$) was chosen. Since BIC is insoluble in hexane, it can be introduced into micellar solution only via the aqueous phase. First it was prepared a stock solution of BIC ($C = 10^{-3}$ M) in water. Then 15 μl of BIC water solution at certain temperature was added to 1 ml of AOT solution in hexane, and the mixture was stirred until formation of transparent microemulsion. The values of w_0 was varied within the range 20÷45 by changing the AOT concentration in hexane from 0.75 to 0.33 M with the amount of aqueous phase being kept constant. Absorption spectra was registered using a microspectrometer USB4000 (OceanOptics, USA) supplied with an incandescent lamp. Luminescence spectra were recorded using Lumina spectrofluorimeter (Thermo Scientific, USA). To decrease scattering influence front-face illumination geometry has been realized using solid sample holder and thin 2 mm quartz cuvette. Luminescence decay spectra were obtained using picosecond spectrofluorimeter FluoTime 200 (PicoQuant, Germany) supplied by green picosecond laser head LDH-P-FA-530 with λ_{em} = 531 nm (PicoQuant, Germany). The width (full width on half-maximum, FWHM) of instrument re-

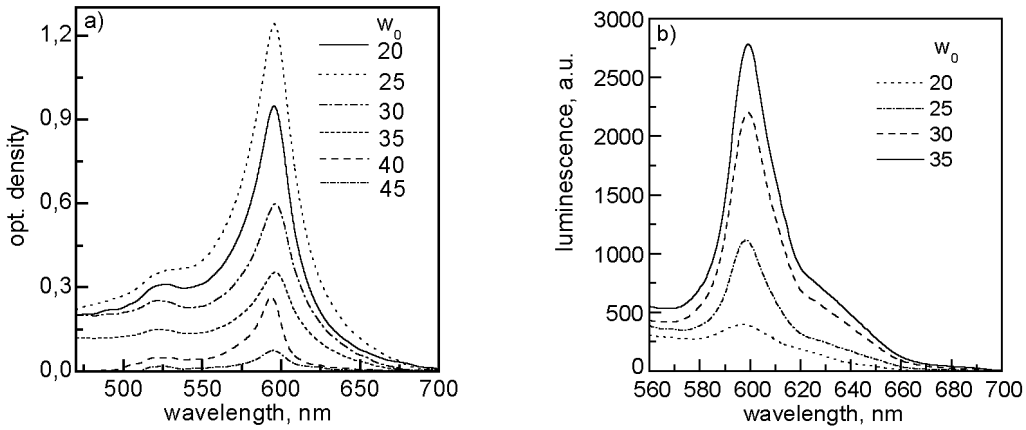

Fig. 2. (a) Absorption and (b) luminescence (λ_{exc} = 530 nm) spectra of BIC *J*-aggregates in AOT RM solutions with different w_0. The temperature of stock water solution at samples preparation was ~ 70°C.

sponse function (IRF) for the spectrofluorimeter was 100 ps. To cut-off laser irradiation an interference long-pass filter HQ565LP (Chroma, USA) has been used. As for steady-state luminescence spectroscopy front-face illumination geometry has been used to decrease the scattering influence. Luminescence decay curves have been deconvoluted using FluoFit software (PicoQuant, Germany). Transmission electron microscopy (TEM) images was obtained using PEM-125K (Selmi, Ukraine) microscope. To contrast organic aggregates 2 % water solution of uranyl acetate was used which was dropped under *J*-aggregates deposited on copper TEM grid. All measurements have been carried out at room temperature if otherwise is not specified.

3. Results and discussion

BIC dye belongs to well-known family of *J*-aggregating 5,5′,6,6′-tetrachlorobenzimidazolocarbocyanine dyes [19]. Due to sulfopropyl groups (see inset in Fig. 1a) it is water-soluble and forms in water *J*-aggregates down to a very small concentrations ($C = 10^{-7}$ M). At the dye concentration $C_{BIC} = 10^{-3}$ M used in our experiments water solution of BIC dye reveals pronounced *J*-band (λ_{max} = 594 nm) and small monomer band (λ_{max} = 516 nm) is seen as a shoulder (Fig. 1a). The luminescence band (λ_{max} = 609 nm) appeared to be strongly red-shifted taking into account very small Stokes shifts which are typical for *J*-aggregates [2–6] including BIC *J*-aggregates [20]. It could be caused by reabsorption due to the large dye concentration and significant extinction coefficient of *J*-aggregates [2–6]. Also it should be noted that at experimental conditions used *J*-band is very wide ($\Delta\nu_J$ = 740 cm^{-1}) and has Lorentz-like long-wavelength tail (Fig. 1a) that is characteristic for large static disorder in *J*-aggregates [21]. For comparison in methanol/water solution (1:4) at $C_{BIC} = 2 \cdot 10^{-4}$ M BIC *J*-aggregates formed on colloidal silver reveal much narrower *J*-band with $\Delta\nu_J$ = 355 cm^{-1} [20]. Despite an intensive study of *J*-aggregate structure for 5,5′,6,6′-tetrachlorobenzimidazolocarbocyanine dyes family using cryo-TEM [22] we haven't found any images of BIC *J*-aggregates for which planar or linear structure has been supposed due to chirality absence [22]. So, we have obtain TEM images of BIC *J*-aggregates and for our surprise found near spherical particles with mean diameter ~ 20 nm (diameter range is 10÷25 nm) (Fig. 1b). Spherical shape is not typical for *J*-aggregates most of which have tubular form [22–24]. Such form could explain high static disorder and absence of chirality which is a feature of tubular aggregates [22]. In spherical aggregates excitons should be delocalized on a strongly curved molecular chains and a quite wide distribution of *J*-aggregates physical sizes should result in a wide distribution of exciton delocalization lengths leading to additional increasing of summary *J*-band width.

So, our task was to prepare BIC *J*-aggregates in reverse micelles. According to the literature data for DEC *J*-aggregates aqueous dyes solution should be heated up to 65–70°C and the better RM sizes are corresponded to that at w_0 = 20÷45 [12–15]. At higher w_0 values water-oil solution sepa-

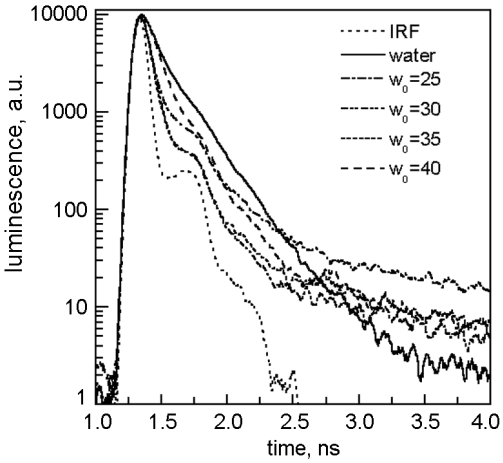

Fig. 3. Luminescence (λ_{exc} = 600 nm) decay curves for BIC *J*-aggregates in water and RM solutions.

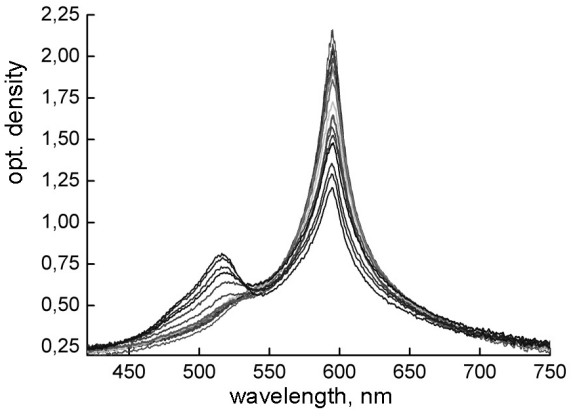

Fig. 4. Absorption spectra of BIC *J*-aggregates in water solution depending on solution temperature. Arrows point to absorption bands changing direction at temperature increasing from 17°C to 95°C.

rates onto individual phases and at lower w_0 values *J*-aggregates appear to be strongly unstable and precipitate [12–15]. Taking into account an expression for water pool diameter for AOT RM ($d = 0.35w_0 + 1.2$ (nm) [14]) the range which has been chosen is corresponding to $d = 8 \div 17$ nm that is lying within BIC *J*-aggregates sizes range.

Absorption and luminescence spectra of BIC *J*-aggregates in RM with different diameters are depicted in Fig. 2. As could be seen from absorption spectra (Fig. 2a) with w_0 increasing intensity of *J*-band becomes to grow and after maximum at $w_0 = 25$ it decreases to the lowest value at $w_0 = 45$. Such behavior of *J*-band dependence on w_0 could be attributed to scattering growth with RM diameter increasing that results in Beer-Lambert law breakdown. Indeed RM solutions appear to be a very turbid and it turbidity grows with RM diameter increasing. Another fact that approve this statement is monotonic decrease of *J*-band width (FWHM) with w_0 growth from $\Delta\nu_J$ = 1090 cm^{-1} at $w_0 = 20$ to $\Delta\nu_J$ = 515 cm^{-1} at $w_0 = 45$ (Fig. 2a). Note that *J*-band width for BIC *J*-aggregates formed in large AOT reverse micelles with $w_0 \geq 40$ appears to be narrower compared to *J*-band width for BIC *J*-aggregates formed in water (Fig. 1a). It could be supposed that in large RMs much more narrow distribution of BIC *J*-aggregates sizes is realized. Contrary to absorption spectra (Fig. 2a) the luminescence spectra reveal growth of intensity with w_0 increasing (Fig. 2b). The main reason for that is front-face illumination geometry of luminescence registering that strongly reduces the scattering influence [25]. Such luminescence growth could be expected due to *J*-band narrowing and resulting oscillator strength increasing [6]. The maximum of luminescence (Fig. 2b) appeared to be blue-shifted compared to water solution case (Fig. 1a). It proves much more narrow distribution of BIC *J*-aggregates sizes in RMs. Note, that at smaller RM diameter cases BIC *J*-aggregates was unstable in RM solution and precipitate during several hours, but at $w_0 \geq 35$ RM *J*-aggregate solutions were stable during several days.

J-band widening with RM diameter decreasing could be attributed both with static disorder increasing [12, 13] and with physical length of *J*-aggregates restricting [14, 15]. To understand what the model is more appropriate in our case we record luminescence decay curves for BIC *J*-aggregates in water solution and RMs with different diameter (Fig. 3). For water solution case the decay curve appears to be not single-exponential and describes by two exponential decays with τ_1 ~ 105 ps (84 %, amplitude weighted) and τ_2 ~ 255 ps (16 %, amplitude weighted) and average lifetime τ_{av} ~ 130 ps (amplitude weighted). According to literature data at room temperature BIC *J*-aggregates have single exponential decay with τ ~ 150 ps [20]. Deviation from single exponential decay in our case could be addressed to exciton localization and trapping on defects due to large static disorder [21]. In RM solutions luminescence decays are also fitted by two exponential curves (Fig. 3). One component is corresponded to a very short

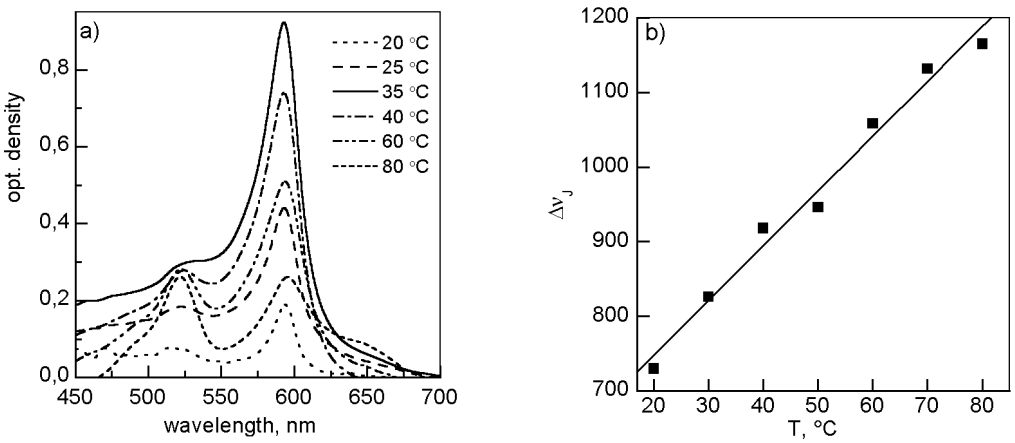

Fig. 5. a) Absorption spectra of BIC *J*-aggregates in AOT RM with $w_0 = 25$ at different stock water solution temperatures. b) *J*-band width (FWHM) dependence on stock water solution temperatures.

decay time which change from $\tau_1 \sim 55$ ps at small w_0 values to $\tau_1 \sim 100$ ps for $w_0 \geq 40$. Second component is corresponded to a very long decay time $\tau_1 \sim 1$ ns which contribution is small (≤ 2 %, amplitude weighted) and decreases with RM diameter growth. The data obtained corresponds to rather static disorder changing case than to physical length restriction case. Indeed, if RM diameter decreasing directly confines physical length of *J*-aggregates we should expect elongation of decay time due to the latter is inversely proportional to exciton delocalization length [6]. Shortening decay time with complex two-component behavior is corresponded to static disorder increasing with luminescence quenching due to exciton localization and trapping effects [21]. It proved by significant increasing luminescence intensity with RM diameter growth (Fig. 2b). Note, that authors of references [14, 15] supposed DEC *J*-aggregates to be just linear chains while such a very simplified structure has never be proved by direct observation using electron microscopy or atomic force microscopy.

The next question is how *J*-aggregates could form in reverse micelles at dye concentrations much smaller than RM concentration. In[14] it was supposed that DEC *J*-aggregates are penetrated to RM water pole as a whole and not to aggregate from monomers as it was supposed by authors in [12, 13]. On other hand at stock water solution temperature of 65–70°C used to prepare RM *J*-aggregate solutions most of *J*-aggregates are fully disaggregated and should to embed into RMs as monomers [26]. To prove BIC dye state at RM formation stage we have obtained thermal destruction spectra for BIC *J*-aggregates (Fig. 4). To our big surprise BIC *J*-aggregates appear to exist even at 95°C with only small contribution of monomer absorption band. Such thermal stability is a very nontrivial and should be addressed to unusual spherical geometry of BIC *J*-aggregates (Fig. 1b). So even for high temperatures of solutions *J*-aggregates dominate under monomers and penetrate into reverse micelles as a whole. Possibly, DEC *J*-aggregates reported early [12–15] have similar structure and thermal stability that explains their formation in RMs at dye concentrations much smaller than RM concentration.

But in such a case possibly another temperature of stock solution will be better for *J*-aggregates preparation within RM water poles. To check it we prepare BIC *J*-aggregates in AOT reverse micelles at different stock solution temperatures (Fig. 5). On example of RMs with $w_0 = 25$ it could be seen that there is the certain stock solution temperature for which *J*-band intensity the biggest (35°C in the case shown on Fig. 5a). Moreover *J*-band width appears to be linear growing with stock solution temperature for BIC *J*-aggregates in AOT RMs (Fig. 5b) pointing to static disorder increasing. At room temperature of stock solution *J*-band width corresponds to that for *J*-aggregates in water even for RMs with $w_0 = 25$. So the better way to prepare BIC *J*-aggregates in RM solution is normal conditions of their preparation.

4. Conclusions

BIC *J*-aggregate formation in AOT reverse micelles has been studied using steady-state and time-resolved spectroscopy.

These *J*-aggregates reveal a very unusual spherical structure and anomalous temperature stability. BIC *J*-aggregates embed into RM water pool as a whole and the better conditions for their embedding is using room or moderate temperatures of *J*-aggregates stock water solutions. Changing RM diameter foremost effects on static disorder in BIC *J*-aggregates with much less influence on their physical sizes.

Acknowledgments. Authors are deeply appreciative to Prof.Yu.V.Malyukin (Institute for Scintillation Materials of NAS of Ukraine) for fruitful discussion of the results obtained. Authors thank to Dr.S.I.Bogatyrenko (V.Karazin Kharkiv National University) for the help with transmission electron microscopy.

References

1. A.Mishra, R.K.Behera, P.K.Behera et al., *Chem. Rev.*, **100**, 1973 (2000).
2. F.Wurthner, T.E.Kaiser, Ch.R.Saha-Muller, *Angew Chem. Int. Ed.*, **50**, 3376 (2011).
3. D.Mobius, *Adv. Matter.*, **7**, 437 (1995).
4. T.Kobayashi (Ed.), *J*-Aggregates, World Scientific Publishing, Singapore (1996).
5. B.I.Shapiro, *Russ. Chem. Rev.*, **75**, 433 (2006).
6. J.Knoester, V.M.Agranovich, in: V.M.Agranovich, G.F.Bassani (Eds.), Electronic Excitations in Organic Based Nanostructures. Thin Films and Nanostructures, Elsevier, Amsterdam, Oxford (2003), v.31.
7. G.Ya.Guralchuk, I.K.Katrunov, R.S.Grynyov et al., *J. Phys. Chem. C*, **112**, 14762 (2008).
8. A.V.Sorokin, I.I.Filimonova, R.S.Grynyov et al., *J. Phys. Chem. C*, **114**, 1299 (2010).
9. I.K.Katrunov, A.V.Sorokin, S.L.Yefimova, Yu.V.Malyukin, *Mol. Cryst. Liq. Cryst.*, **535**, 57 (2011).
10. S.Yefimova, A.Lebed, A.Sorokin et al., *J. Mol. Liq.*, **165**, 113 (2012).
11. A.V.Sorokin, I.I.Fylymonova, S.L.Yefimova, Yu.V.Malyukin, *J. Phys. Conf. Ser.*, **345**, 012047 (2012).
12. A.S.Tatikolov, S.M.B.Costa, *Chem. Phys. Lett.*, **346**, 233 (2001).
13. A.S.Tatikolov, S.M.B.Costa, *Photochem. Photobiol. Sci.*, **1**, 211 (2002).
14. L.M.Nikolenko, A.V.Ivanchihina, S.B.Brichkin, V.F.Razumov, *J. Coll. Interf. Sci.*, **332**, 366 (2009).
15. L.M.Nikolenko, S.B.Brichkin, T.M.Nikolaeva, V.F.Razumov, *Nanotech. Rus.*, **4**, 19 (2009).
16. V.Uskokovic, M.Drofenik, *Surf. Rev. Lett.*, **12**, 239 (2005).
17. J.Eastoe, M.J.Hollamby, L.Hudson, *Adv. Coll. Interf. Sci.*, **128–130**, 5 (2006).
18. M.P.Pileni, *J. Exp. Nanosci.*, **1**, 13 (2006).
19. A.Pawlik, A.Ouart, S.Kirstein et al., *Eur. J. Org. Chem.*, **2003**, 3065 (2003).
20. S.Ozcelik, I.Ozcelik, D.L.Akins, *Appl. Phys. Lett.*, **73**, 1949 (1998).
21. Yu.V.Malyukin, O.G.Tovmachenko, G.S.Katrich, *Low Temp. Phys.*, **24**, 879 (1998).
22. S.Kirstein, S.Daehne, *Int. J. Photoenergy*, **2006**, Article ID 20363 (2006).
23. H.von Berlepsch, C.Bottcher, L.Dahne, *J. Phys. Chem. B*, **104**, 8792 (2000).
24. E.Lang, A.Sorokin, M.Drechsler et al., *Nano Letters*, **5**, 2635 (2005).
25. J.R.Lakowicz, Principles of Fluorescence Spectroscopy, 3rd ed. Springer, New York, Singapore (2006).
26. Yu.V.Malyukin, S.L.Efimova, A.V.Sorokin, A.M.Ratner, *Functional Materials*, **10**, 715 (2003).

Формування *J*-агрегатів у разчинах зворотних міцел

І.І. Филимонова, С.Л. Ефімова, О.В. Сорокін

Досліджено особливості формування *J*-агрегатів ВІС у розчинах зворотних міцел (ЗМ) за допомогою стаціонарної спектроскопії оптичного поглинання та люмінесцентної спектроскопії, а також люмінесцентної спектроскопії, що розподілена у часі. *J*-агрегати ВІС мають сферичну геометрію з діаметром близько 20 нм, а також виявляють значну температурну стабільність. Зменшення діаметра зворотних міцел призводить до збільшення статичного безладу, в результаті чого відбувається розширення *J*-смуги і збільшення інтенсивності люмінесценції. Завдяки високій температурній стабільності, *J*-агрегати ВІС вбудовуються в ЗМ при будь-яких температурах вихідного розчину. Зменшення температури вихідного розчину призводить до звуження *J*-смуги і збільшення її інтенсивності внаслідок зменшення статичного безладу.